



**HAL**  
open science

# Deep Learning for Enrichment of Vector Spatial Databases: Application to Highway Interchange

Guillaume Touya, Imran Lokhat

► **To cite this version:**

Guillaume Touya, Imran Lokhat. Deep Learning for Enrichment of Vector Spatial Databases: Application to Highway Interchange. ACM Transactions on Spatial Algorithms and Systems, 2020, 6 (3), pp.21. 10.1145/3382080 . hal-02465244

**HAL Id: hal-02465244**

**<https://hal.science/hal-02465244v1>**

Submitted on 3 Feb 2020

**HAL** is a multi-disciplinary open access archive for the deposit and dissemination of scientific research documents, whether they are published or not. The documents may come from teaching and research institutions in France or abroad, or from public or private research centers.

L'archive ouverte pluridisciplinaire **HAL**, est destinée au dépôt et à la diffusion de documents scientifiques de niveau recherche, publiés ou non, émanant des établissements d'enseignement et de recherche français ou étrangers, des laboratoires publics ou privés.



Distributed under a Creative Commons Attribution 4.0 International License

---

# DEEP LEARNING FOR ENRICHMENT OF VECTOR SPATIAL DATABASES: APPLICATION TO HIGHWAY INTERCHANGE

---

A PREPRINT

**Guillaume Touya**

LASTIG, Univ Gustave Eiffel, IGN, ENSG  
Saint-Mandé, F-94160  
guillaume.touya@ign.fr

**Imran Lokhat**

LASTIG, Univ Gustave Eiffel, IGN, ENSG  
Saint-Mandé, F-94160  
imran.lokhat@ign.fr

February 3, 2020

## ABSTRACT

Spatial analysis and pattern recognition with vector spatial data is particularly useful to enrich raw data. In road networks for instance, there are many patterns and structures that are implicit with only road line features, among which highway interchange appeared very complex to recognise with vector-based techniques. The goal is to find the roads that belong to an interchange, *i.e.* the slip roads and the highway roads connected to the slip roads. In order to go further than state-of-the-art vector-based techniques, this paper proposes to use raster-based deep learning techniques to recognise highway interchanges. The contribution of this work is to study how to optimally convert vector data into small images suitable for state-of-the-art deep learning models. Image classification with a convolutional neural network (*i.e.* is there an interchange in this image or not?) and image segmentation with a u-net (*i.e.* find the pixels that cover the interchange) are experimented and give results way better than existing vector-based techniques in this specific use case.

**Keywords** spatial data enrichment · deep neural networks · highway interchange · map generalization

## 1 Introduction

Spatial analysis of vector data remain very complex because of the diversity of configurations and the heterogeneity of datasets. Among other applications, map generalization, *i.e.* the process to simplify map information when scale is reduced, is particularly dependent on vector pattern recognition [1] to make explicit the implicit structures of the map (*e.g.* buildings aligned along a road). This vector pattern recognition task is very complex and the existing techniques are not completely satisfying. Pattern recognition in images was recently revolutionized by deep convolutional neural networks (CNNs) and more generally deep learning techniques. Even if CNNs cannot directly work on vector data for now, can they also revolutionize vector spatial analysis?

Deep learning has already been thoroughly used on spatial information but generally on raster spatial information or on 3D point clouds: for style transfer, *e.g.* a Google Earth image rendered as a Google Maps image [2, 3], for image segmentation, *i.e.* finding buildings, roads, crosswalks or other features in images [4, 5, 6], or for image classification [7, 8, 9]. But it is also possible to use deep learning techniques when vector spatial data is concerned, with images generated from representations of the vector data: the machine learning model learns to process the images of the vector data, and not the vector data themselves. Applications to the assessment of OpenStreetMap data quality [10], car trajectory analysis [11], or map generalization [12, 13] were recently proposed. This papers follows the same principles, *i.e.* generating images of the vector data, to explore the possibilities offered by deep learning for vector spatial analysis. The workflow is the following: first convert vector data to raster optimally, then process the raster data with deep learning techniques, then finally reinject the results into the vector dataset. The paper focuses on a use case that is particularly difficult to tackle with vector data analysis: automatically identifying the road sections that belong to a highway interchange.

This paper is structured as follows: Section 2 describes more the use case and the past attempts using vector-based or geometrical spatial analysis. Then, Section 3 presents an image classification model that identifies images containing highway interchanges. Section 4 details an image segmentation model that identifies the pixels of the image containing highway interchanges. Then, Section 5 discusses the optimal generation of training images based on vector spatial data. Finally, Section 6 draws some conclusions and discusses future research.

## 2 Highway Interchange Detection in Vector Datasets

Usually, roads are modelled in geographic datasets with minimal semantics. But they are important features of most maps, not only topographic maps, because of their key role for transportation. This is why road network enrichment by spatial analysis has been an important topic for years in geographic information science [14, 15, 16, 17, 18, 19]. Past research focused on various types of road structures and patterns: continuous road sections or strokes [16], complex crossroads [15, 18], ring roads [14, 17], grid-like patterns [14, 17, 19], dual carriageways [19], etc.

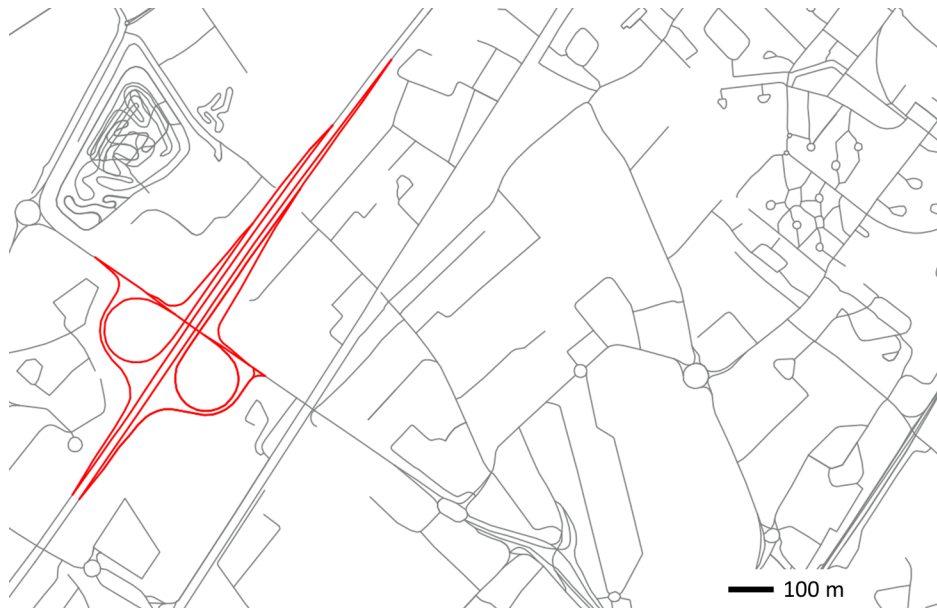


Figure 1: Illustration of the use case: finding the roads sections that belong to a highway interchange (in red here).

Among these patterns and structures that are implicit in a network of road sections, highway interchange are particularly interesting (Figure 1). Highway interchange road sections are the roads that connect a highway with other highways or other simple roads. Highway interchange patterns can be very diverse, and even if most of them can be classified to well-known patterns [20], local modifications of the patterns make them hard to recognize. Why do we need to detect highway interchange roads? The main application is map generalization, because highway interchange can be represented very differently across scales (Figure 2), and a generalization process requires the identification of these patterns prior to their graphical abstraction [21, 22]. The recognition of highway interchange is also useful to enrich data in car navigation application [20].

In order to detect the roads belonging to an interchange, road directions can be effectively used as slip roads and highway sections are mainly one-way directed [23]. The shape and the curvature of the road sections can also be used to detect interchanges [18], but in this work, the road network is already limited to highway sections plus slip roads thanks to an attribute value in the road dataset.

When there is no semantic information on road direction or road function, two other methods exist in the literature to recognize the road sections that belong to a highway interchange, the second one being a specialization of the first one [21, 22]. The method is based on the classification of each junction between two road sections according to their shape and their connectivity. For instance, *y-shaped* junctions are connected with three road sections that form angles similar to the shape of letter *y*. The first step of the detection method is to recognize the *y-shaped* or *fork-shaped* junctions. Then, the second step is to cluster the close detected junctions using the distance in the road network as the clustering distance. Then, all the roads intersecting the convex hull of the large clusters are considered as belonging to a highway interchange.

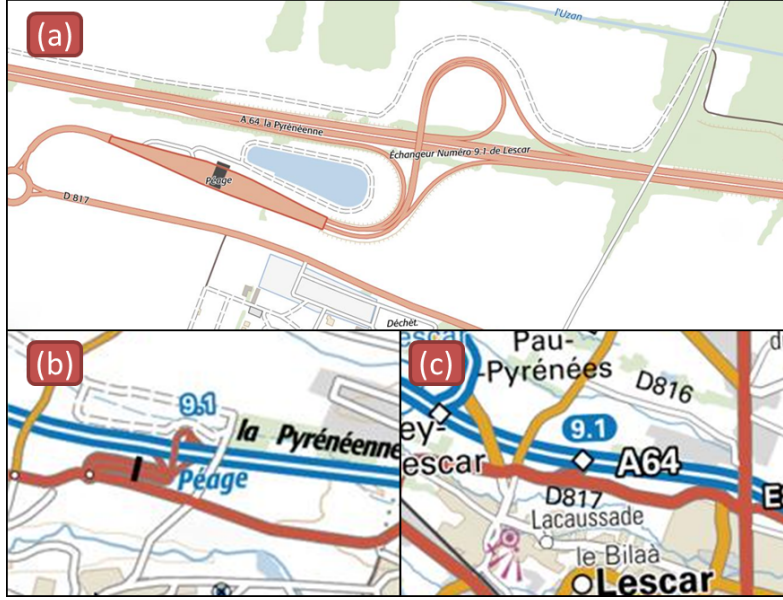


Figure 2: (a) Highway interchange fully represented with road sections at the 1:10k scale. (b) The same interchange topologically represented at the 1:100k scale. (c) The same interchange represented with a point symbol at the 1:250k scale.

In this use case, the road data we work with is produced by the French national mapping agency<sup>1</sup>, and covers the whole French territory. In addition to the polylines, the road sections are labeled with an importance value that distinguishes highways from less important roads, but the sliproads that connect the network to the highway have varying importance values, which prevents from using this semantic information in the detection (Figure 3). In this dataset, we can also find an interesting geographic layer with the large complex junctions, which include some highway interchange, being represented with a point geometry (Figure 3). This multiple representation of highway interchange is a key feature to automatically derive training datasets for machine learning [13]. But only approximately half of the French highway interchange are considered as large junctions, so this information cannot really be used in the vector-based detection method.

Figure 4 shows some results on the use case dataset with the existing vector-based method from [22]. The results are generally unsatisfying. Around 40% of the interchange are correctly delineated, as in Figure 4a, but most interchange instances are identified but incorrectly delineated, as in Figure 4b; there is even a significant part of the detected interchange instances that are in fact not highway interchange as in Figure 4c. These results confirm that a better method is required and the paradigm shift brought by CNNs gives that better method as shown in the following section.

### 3 Detection by Image Classification

#### 3.1 Classification of Road Network Images

The initial breakthrough of deep learning models was in the domain of image classification, so our first idea was to classify small images of the road network to classify them into two classes: *interchange*, which means there is at least one instance of interchange in the image, and *no interchange*, which means that there is no instance of interchange in the image. Such a modelling of our problem does not provide the road sections that belong to an interchange. But if the image is small enough, it should limit the parts of the network that are processed with the vector-based method, and could improve its results. At least, it should avoid the false positive instances like the one in Figure 4c.

Our problem is reduced to an image classification problem, so we decided to use a deep convolutional neural network (CNN) that proved successful for such problems. We empirically selected a network close to LeNet-5 network that was proposed for hand-drawn digits recognition [24]. The version of the network we used is described in Figure 5. It can be noted that we added a dropout layer that reduces over-fitting, which was particularly important for the *no-interchange* images that can be more diverse than the ones with interchange, so the training images might not represent the diverse

<sup>1</sup>IGN, <http://www.ign.fr>

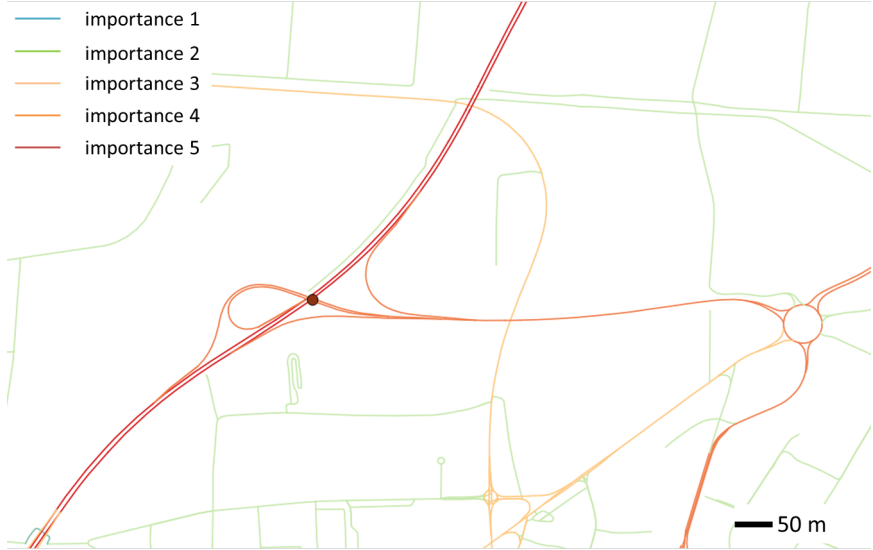


Figure 3: The initial vector dataset for the use case: detailed roads, with an importance value conveyed by the color in the image (red is the most important). There are also points for a small part of the highway interchanges.

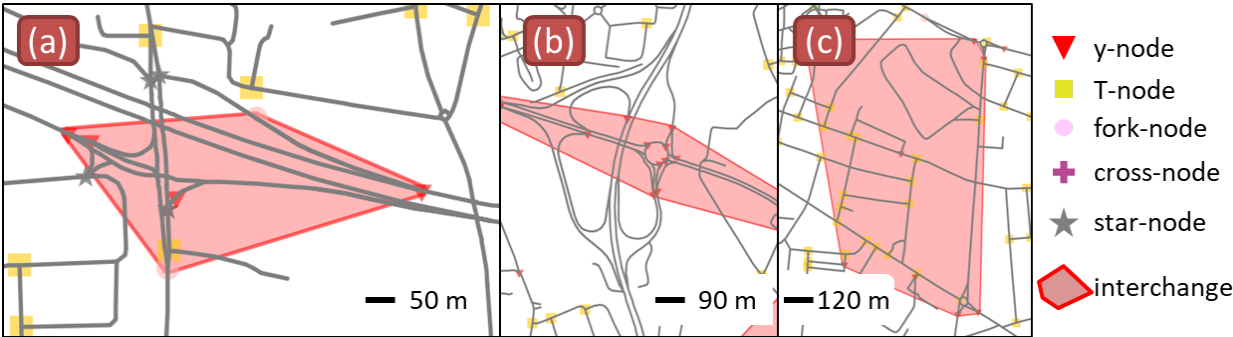


Figure 4: Results of the method from [22]: (a) interchange correctly delineated; (b) interchange identified but incorrectly delineated; (c) interchange identified where there is no interchange. The symbols represent the classified crossroads.

patterns with enough instances. A dropout layer randomly drops out some of the units of the network to prevent co-adaptations during the early steps of training [25]. Table 1 shows the parameters used in the CNN.

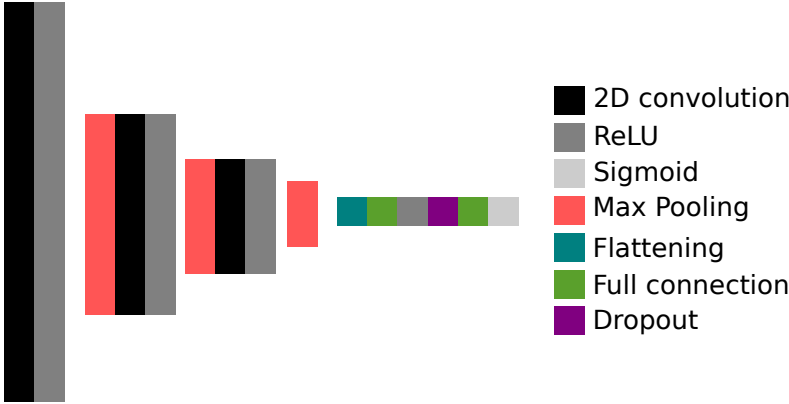


Figure 5: Architecture of the convolutional neural network used to classify interchange images.

| Layer           | Kernel or pool size | Strides |
|-----------------|---------------------|---------|
| convolution 2D  | 32 x 32             | 3 x 3   |
| maximum pooling | 2 x 2               | -       |
| convolution 2D  | 64 x 64             | 3 x 3   |
| maximum pooling | 2 x 2               | -       |
| convolution 2D  | 128 x 128           | 3 x 3   |
| maximum pooling | 2 x 2               | -       |
| convolution 2D  | 128 x 128           | 3 x 3   |
| maximum pooling | 2 x 2               | -       |
| flatten         | -                   | -       |
| fully connected | 64                  | -       |
| fully connected | 64                  | -       |
| dropout         | 0.5                 | -       |
| fully connected | 1                   | -       |

Table 1: Model architecture of the proposed CNN. H and W are the height and the width of the input image

### 3.2 Generating a Training Dataset

As mentioned earlier, the dataset for this use case is composed of road line sections that cover the whole French territory, and of 2835 point that correspond to the most significant highway interchange of the country. We also have access to a complete topographic dataset, and we will see later that it will be useful to automatically generate the training dataset for our model.

The first step is to generate the instances of the first class, *i.e.* the *interchange* images. We use the 2835 points to generate the same number of images of the *interchange* class. We generate images with 256\*256 pixels with a scale of 1.2 \* 1.2 km per image (Figure 6). This couple of values for image size and scale gives a good compromise between images that should be big enough to contain all the interchange roads, but small enough to make the vector-based detection effective. The images are centered on the interchange point, and then randomly slightly deviated from the center, as the images that the model will predict after training might contain interchanges near their border. We decided to generate black and white images with the background in black and the roads in white, with a 1 pixel width as road symbol. All these choices to generate the images are discussed in Section 5.

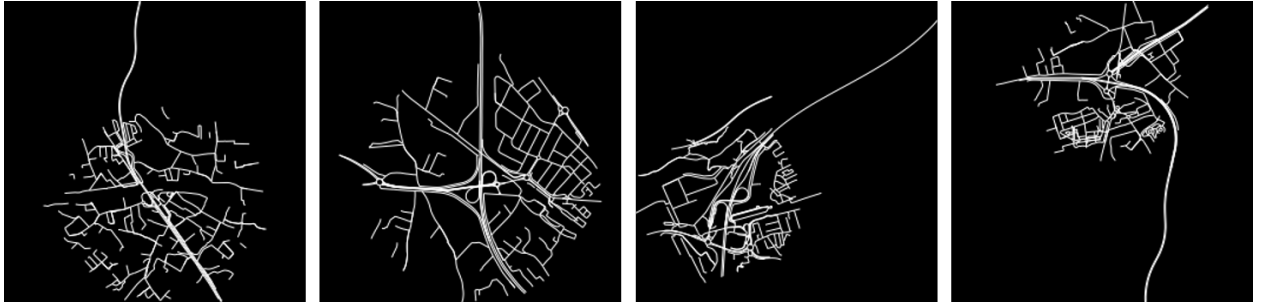


Figure 6: Four sample images containing a highway interchange, used to train the model to recognize images.

Then, the second step is to generate the training examples of the second class, *no-interchange*. We need to generate images that do not contain any interchange. Rather than picking some random points in our road network, a more controlled process was used. First, tunnel points available in the dataset were extracted, and only the ones that do not have an interchange point around were kept. Images were generated with the same process as with interchange points (Figure 7). The number of these points was not big enough, and the road network around tunnels, mostly located in mountainous areas, did not represent well the diversity of network structures. Then, school points that do not have an interchange point around were used, in order to have more points with more diverse network structures (Figure 8). Using these points, 3410 images were generated for the class *no interchange*.

In terms of implementation, scripts using the Mapnik library<sup>2</sup> were developed to interact with the data stored in a PostGIS database. Mapnik is a library to generate tiled raster maps from geographic information, and can be easily hacked to generate images for deep learning.

<sup>2</sup><https://mapnik.org>

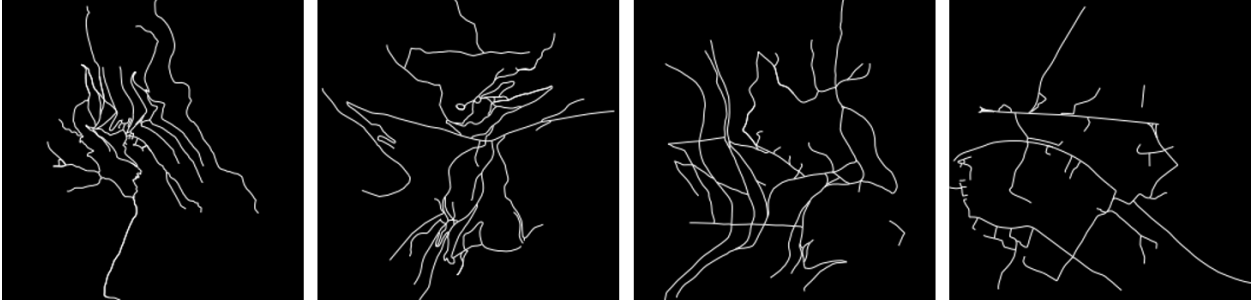


Figure 7: Four sample images containing a tunnel, used to train the model to recognize images without interchange.

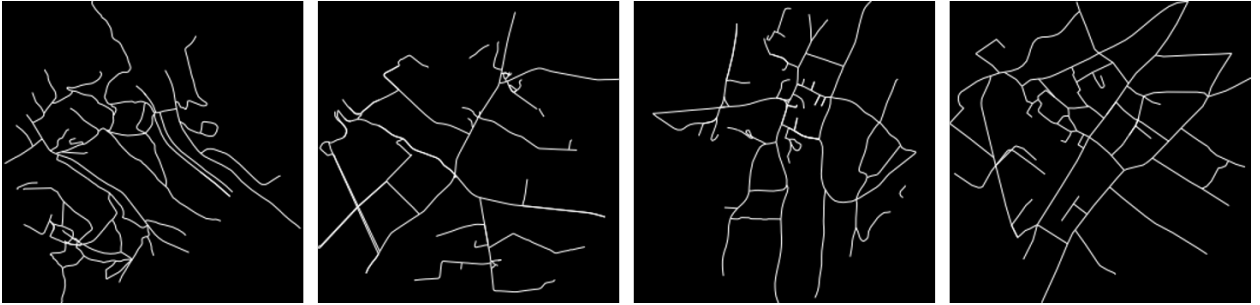


Figure 8: Four sample images containing a school, used to train the model to recognize images without interchange.

In order to process the vector data that is classified in the *interchange* class, keeping track of the original vector data, related to a given image, is necessary. Several options are possible: generating a geotiff image, *i.e.* a geolocated image, or keeping track of the coordinates of the extent of each image in a separated file. We chose a third option and generated a geojson file containing the vector data related to each training image, using the same Mapnik library. The created training dataset will be made openly available, as well as the scripts and the model, in the following weeks.

### 3.3 Results

To test the model and the training dataset, we separated the images of each class randomly, keeping a little more than 1500 images in each class for the training phase, 500 in each class for testing during the training phase, and another 500 images in each class for a further assessment of the trained model. The presented results in this sub-section are all from these last 500 images of interchange and 500 without interchange. The model was implemented with the Keras Python library, with a TensorFlow core.

The best results obtained with this dataset were ceiling around 96% of overall accuracy on the test data, so we added some data augmentation with random rotation of the input images, which yielded better results with 99.6% of overall accuracy, with a loss of 0.036, on the test data. The detailed results presented in Table 2 show that images containing interchange instances are correctly classified with an even higher rate of 99.8%, which means that images without interchange are classified as false positive 0.8% of the time. This results is interesting because the aim of this classification model was not to provide an automated result for interchange detection, but just a optimised subset of the road network to improve the vector-based method, and this is what is achieved with this model.

The best results were obtained with a batch size of 64 and 100 epochs. To select these optimal values, experiments were carried out with batch sizes ranging from 16 to 128, and epochs ranging from 20 to 500.

In order to assess how good this model performed, there is no existing baseline, so we defined two ourselves. The first one is based on the vector-based method: the vector-based interchange detection is triggered on each vector extract corresponding to an image of the validation dataset and the extract is classified as "interchange" when there is at least one interchange instance detected, and "no-interchange" when there is none. The results of this baseline are presented in Table 3. The CNN classifier is clearly better than the vector baseline and the difference is even bigger, as expected, on the images that do not contain any interchange.

The second baseline is also analysing the vector data and not its image, and uses a random forests classifier. We derived a set of descriptors of the vector road sections in each extract of the dataset. The random forests classifier was trained

| Classification \ Label                        | interchange                     | no-interchange |
|---|---------------------------------|----------------|
|   | % of interchange classification | 99.8%          |
| % of no-interchange classification            | 0.2%                            | 99.2%          |
| number of images classified as interchange    | 499                             | 4              |
| number of images classified as no-interchange | 1                               | 496            |

Table 2: Confusion matrix of the best classification result obtained with the proposed model trained with our training examples.

| Classification \ Label                        | interchange                     | no-interchange |
|---|---------------------------------|----------------|
|   | % of interchange classification | 81%            |
| % of no-interchange classification            | 9%                              | 66.2%          |
| number of images classified as interchange    | 405                             | 169            |
| number of images classified as no-interchange | 95                              | 331            |

Table 3: Confusion matrix of the classification results obtained with the vector baseline.

with the same train and test datasets, and then assessed on the same validation dataset. We used the following descriptors in our baseline:

- the number of intersections (as interchanges contain a high density of intersections);
- the total length of roads in the extract (to describe the global density of the network);
- the mean and the standard deviation of the road sections lengths;
- the mean and standard deviation of the road sections sinuosity (the proxy for sinuosity used here is the distance between the extreme points of the polyline divided by the length of the polyline);
- the total length of the road sections with maximum importance (as highways are mainly labeled with a maximum importance).

This second baseline gives an accuracy of 88.3% on the 500 extracts of the validation dataset, and the confusion matrix is presented in Table 4. The results of the second baseline are already way better than the first one, but once again, our proposed CNN model clearly outperforms this baseline. We believe that the ability of the CNN to detect the cluttered areas of the image explain the performance difference as the descriptors used in this baseline are not really able to convey this local clutter caused by the rendering of interchange road sections.

| Classification \ Label                        | interchange                     | no-interchange |
|---|---------------------------------|----------------|
|   | % of interchange classification | 87.4%          |
| % of no-interchange classification            | 12.6%                           | 89.2%          |
| number of images classified as interchange    | 437                             | 54             |
| number of images classified as no-interchange | 63                              | 446            |

Table 4: Confusion matrix of the classification results obtained with the random forests baseline.

We also used the Grad-CAM algorithm [26] to visually assess what was learned by the CNN. Figure 9 shows heatmaps that correspond to what "sees" the last layer of the CNN, and it clearly learns to highlight the locations of the interchange, which confirms the good classification results.

### 3.4 Detecting Interchange Roads in Predicted Images

Now that the classification gives a subset of the road network that is very likely to contain highway interchange instances, we need to check that it improves the vector-based method results. We processed all the extracts that were related to an image classified as *interchange*, analyzed the results. Although, there is a major improvement compared to a the initial processing of the complete road network, the results are still unsatisfying (Figure 10).

It is pretty clear that both the classification results and the vector-based detection could be improved, by adapting the method to process small extracts of the network that do contain an interchange instance. We believe that the way to



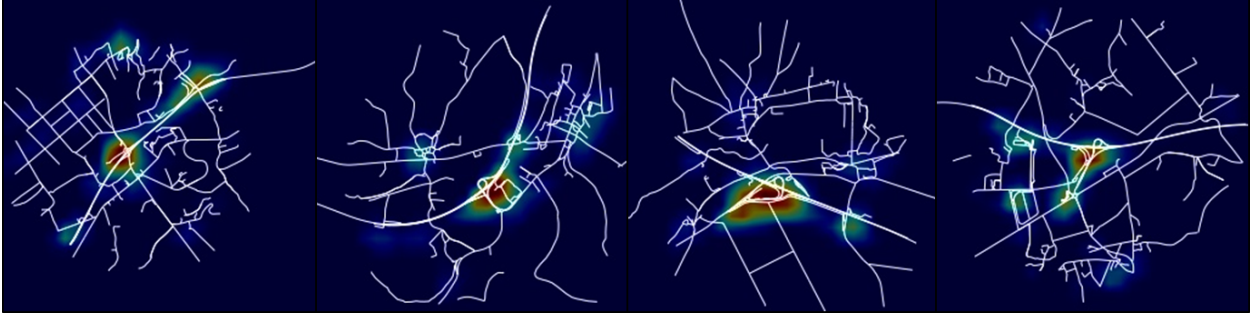


Figure 9: Four sample heatmaps that visually illustrate what the last layer of the CNN "sees", based on the Grad-CAM algorithm [26]

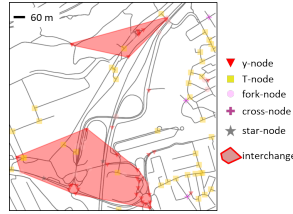


Figure 10: Vector-based detection algorithm used on the roads extracted from an image classified as highway interchange: the interchange is detected but with two different parts, the middle sections being left undetected.

optimize our results is to both filter even more the roads to process in the vector method, and to adapt the vector method to these filtered roads. In this paper, we decided to first focus on filtering even more the roads on which to apply the vector-based method. We propose to use an image segmentation model, and this segmentation method is presented in the following section.

## 4 Detection by Image Segmentation

### 4.1 Segmentation of Road Images

Image segmentation by deep learning has been a very active field in the past ten years, and models are now able to delineate features in photographs, scientific images or videos. The images generated from the road network are not close to photographs that attract most of the attention of the researchers, but closer to the scientific images processed in the papers introducing the U-Net architecture [27]. U-Nets were already used with images generated from vector spatial data [12, 11]. U-Nets provide a classification probability for each pixel of an input image, and are based on a sequence of down convolutions, as in CNNs, and then up convolutions (Figure 11). The compactness of the features segmented by the model is assured by so-called *concatenate* layers that are connected to the neurons of down convolution layers.

We also briefly tried other network architectures dedicated to segmentation problems [28, 29], but there was no clear improvement compared to our U-Net, so we decided to limit the investigations with these networks. Future work is required to know if a finer architecture can improve our results.

### 4.2 Generating a Training Dataset

In this case, a training example consists in an input image of the road network and a label image showing the pixels of the input image that belong to an interchange (Figure 12). We first used the same images as the ones in the classification model, but the results were not optimal so we changed the color model only, switching from black and white images to RGB images, with a white background and roads with colors corresponding to their importance value in the dataset. As highway interchange are usually around important roads, it helped improving the segmentation results a lot.

Regarding the label images, they are black and white images where a white pixel means that the pixel does not belong to an interchange, and a black one means that the pixel belongs to an interchange. The label images were generated from the interchange points used to train the classification model, and a black square was generated around each point. The size of the square is kept rather small to make sure it does not cover areas where there is no interchange. The

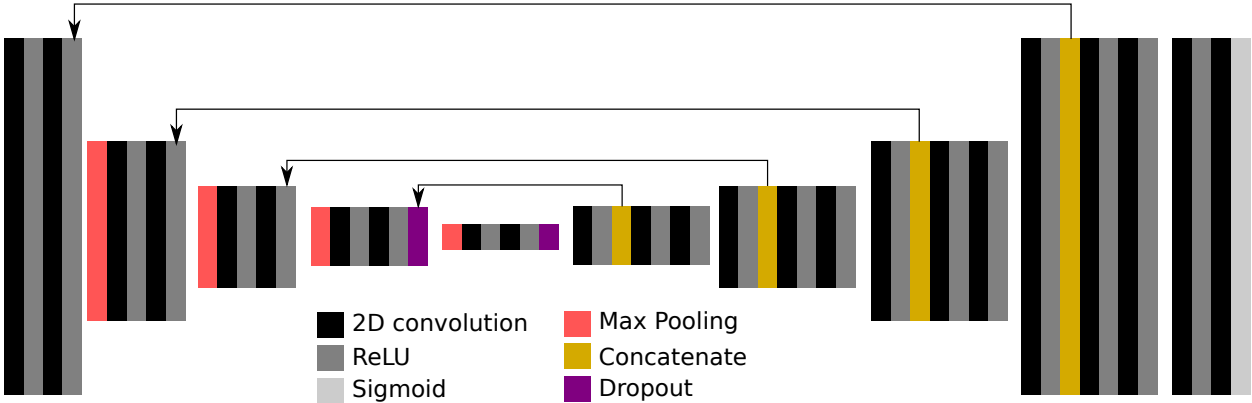


Figure 11: Architecture of the U-Net used for the segmentation of interchange images. The arrows show how the concatenate layers are connected to previous layers of the model.



Figure 12: Four examples used to train the segmentation model. In the input images on top, the colors are related to the importance value of each section (red is most important, and black is least important). In the label images below, a black square is generated around the interchange points.

drawback is that it does not completely cover all the roads of the interchange. Label images that do not contain any interchange are left totally white.

### 4.3 Results

The experiment setup was the same as the one for image classification: similarly to the classification experiment, we separated the images of each class randomly into train, test, and validation datasets; and the U-Net model was also implemented with the Keras Python library, with a TensorFlow core.

The best results obtained after 30 epochs are the following: an accuracy of 97.8% and a loss value of 0.0696 on the training data, and an accuracy of 94.3% and a loss value of 0.3773 on the validation data.

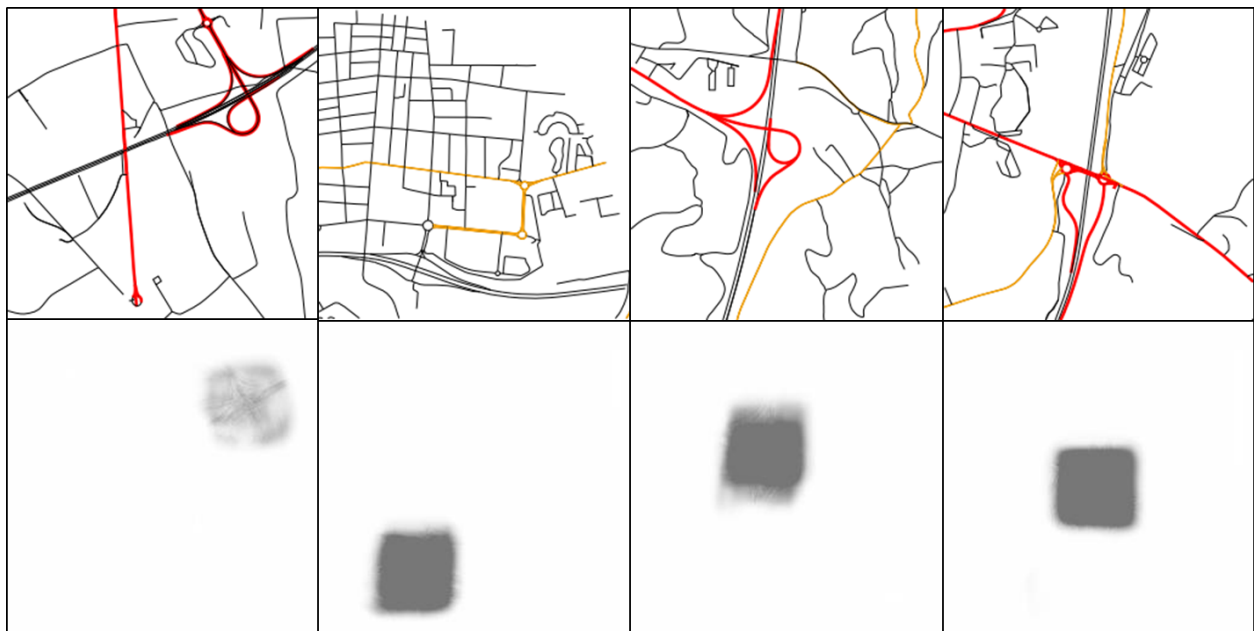


Figure 13: Results of segmentation: the input images (top), and the predicted segmentation (bottom). Darker shades of grey correspond to higher probabilities of being part of the interchange.

Figure 13 shows some good results on four of the interchange images of the test data. The pixels with the higher probabilities (with darker shades of grey in the image) are clearly the ones that intersect the roads of the interchange. Even the very small interchange on the right of the image is correctly segmented. Even when the highway is not colored in red because the importance value is not the one usually applied to such roads (maybe an error in the data), the interchange is segmented (second image from the left). Similar good results appear on a large majority of the tested samples: sometimes, the pixels with a high probability cover a little more than the interchange, and sometimes they cover a little less, but as the raster-based segmentation is just a first step to filter the roads to included into the vector-based method, the results really correspond to what was expected. Figure 14 shows four other examples that confirm the good results even with very complex or unusual structures. The image from the right shows the correct segmentation of two different interchanges in the same image. And the third image shows that there is nothing segmented when there is no interchange in the image.

However, both figures show that the segmented area is always mostly a square due to the shape we gave to our training masks. In the examples of figures 13 and 14, the square grossly captures the interchange location, but in some rare cases, the delineation is visually not correct. We compared the segmentation results with interchange delineations performed manually in Figure 15. Sometimes, the segmented square is not located on the interchange (in the left image, the model segmented the roundabout instead of the small interchange at the bottom left). And sometimes, the square is off-center (in the other three images).

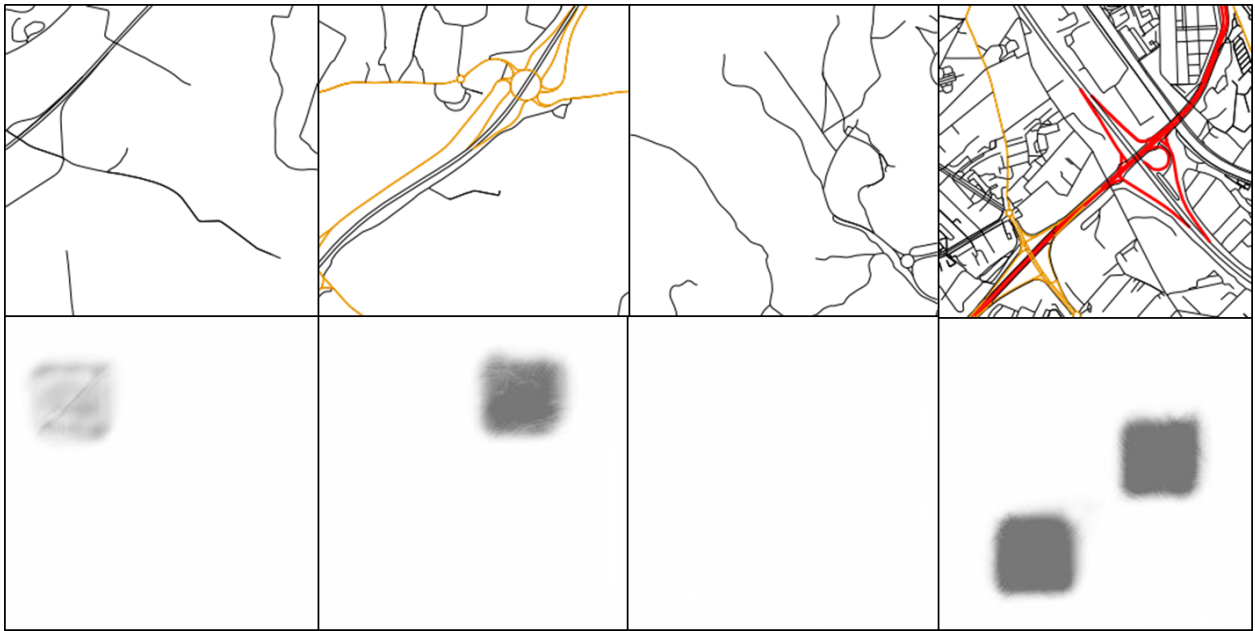


Figure 14: Other results of segmentation: the input images (top), and the predicted segmentation (bottom). Darker shades of grey correspond to higher probabilities of being part of the interchange.



Figure 15: Results of segmentation compared with handdrawn interchange delineation.

## 5 Deriving Training Images from Vector Spatial Datasets

The previous two sections presented two deep learning models to detect highway interchanges in road networks that we trained with images derived from vector data. The way images are generated was determined empirically, and it might be sub-optimal. There are different variables on image generation: the scale and the resolution of the image, the style of the rasterized vector data, data selection, and the way the label area is created in the segmentation use case. In this section, we discuss different alternatives for these variables to generate the training images from vector data, and how they perform in our use cases.

### 5.1 Scale and Image Resolution

The first two variables to set when generating images for the vector data are the scale and the resolution of the image. The scale is simply the ratio between the width (or height) of the image and the length of the same geographic extent on the ground. The image resolution is the ratio between the width (or height) of the image and the number of pixels.

In order to assess the importance of those two variables on the effectiveness of the images, we tested two types of variations:

- scale variations: same image size and resolutions, but different ground extents;
- resolution variations: at constant scale, different image resolutions by changing the number of pixels (128x128, 256x256, 512x512).

Table 5 shows the results obtained with resolution variations with the image classification model, for a same scale (images cover 1.2 km x 1.2 km). The resolution we used (256 x 256 pixels) gives the best results. A smaller resolution gives worse results, but they are still very good. On the contrary, a larger resolution gives much worse results, which suggests that images should not be larger than 256 x 256 pixels. A smaller resolution than 128 x 128 pixels for such a scale was not tested but we believe that it would give bad results as many highway interchanges would be covered by very few pixels, making them hard to recognise in the image.

| resolution | accuracy | loss  | interchange ratio | no-interchange ratio |
|------------|----------|-------|-------------------|----------------------|
| 128 x 128  | 98.6%    | 0.098 | 496/500           | 491/500              |
| 256 x 256  | 99.8%    | 0.036 | 499/500           | 496/500              |
| 512 x 512  | 95.6%    | 0.328 | 486/500           | 466/500              |

Table 5: Classification results with training images of different sizes for a same geographic extent.

The scale variation was also tested but the range for scale variation in our use case is not that big. Hence, an highway interchange can be quite large and a too large scale might cause incomplete interchanges in the images, which is a problem. On the other hand, too small scales might cause too much coalescence between the road symbols, except if the resolution is high enough (but we have seen just before that a high resolution gives bad results). This is why only slight variations of the scale were tested: Figure 16 shows images that are 1.2 km wide and images that are 0.8 km wide. The results with these two scales are extremely similar, so we conclude that if scale remains in a reasonable range, this variable has a low impact on the effectiveness of the deep learning models.

### 5.2 Styling Vector Data

Besides scale and resolution, another key variable is the way vector data is styled prior to rasterization. In the experiments described in the previous sections, we tested two different styles:

- a black background and white symbols for roads (1 pixel width);
- a white background and roads colored according to importance (from black to red, with 1 pixel width).

The first style has the advantage of simplicity, as the color information is coded with only two values 0,1 while a colored are coded with a triplet of values between  $[0, 256]$ . The drawback of this simple style is that it does not use the semantic information about the roads importance, while highways are coded as important roads. It was enough to get great classification results but not enough for the segmentation model.

The second style makes a complete use of the convolutional layers, as the model learns that interchange roads often lie around roads colored in red (the color of the most important roads). However, we have seen in the results that not

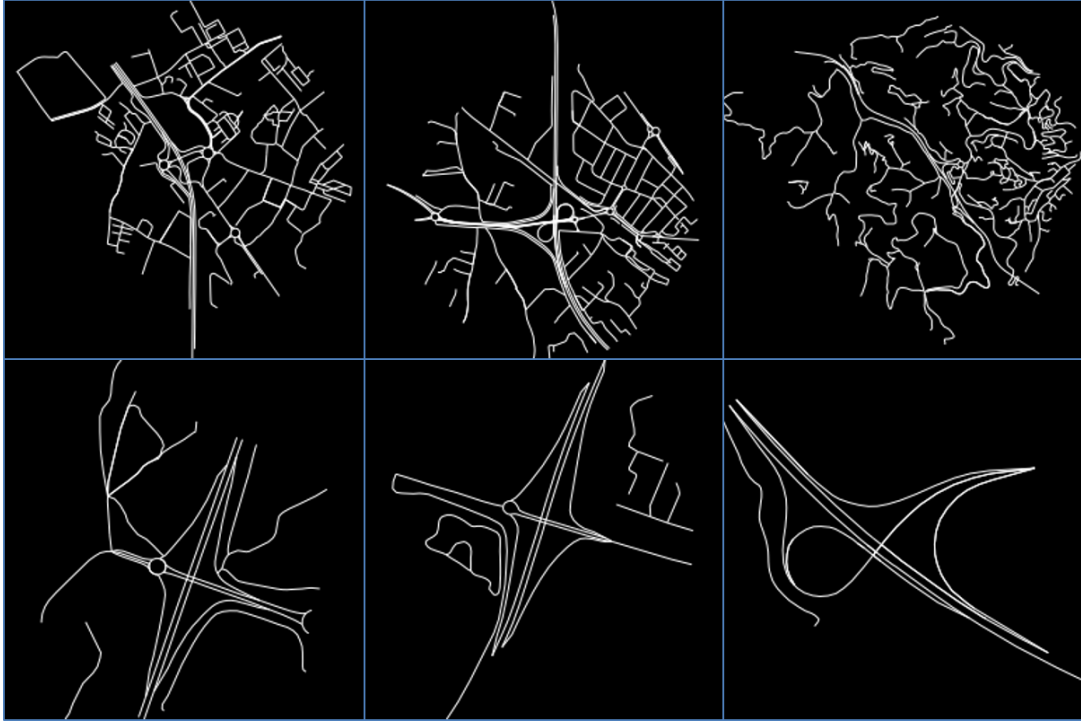


Figure 16: Two series of images with a different extent for the same image size: the extent is larger in the top images than in the bottom images.

all interchange instances contain roads coded as important (Figure 14), so we have to make sure that colors do not introduce a learning bias.

Another way to modify style is to change the width of the symbols applied to roads, rather than the colors. Figure 17 shows an example of an interchange represented with a symbol width of 1 pixel on the left, and two pixels on the right. It is visually clear that a symbol width of 2 pixels introduces symbol coalescence, and this coalescence might blur the location of interchanges. A quick test on the classification model with 2 pixels symbols confirmed our doubts, with much lower classification results. However, this quick test does not dismiss the usefulness of using larger widths for other use cases where a larger scale is possible.



Figure 17: Two images generated with a road symbol width of 1 pixel on the left and 2 pixels on the right.

### 5.3 Data Selection

The last variable for the generation of input images is selection of the features of the dataset to render in the image. First, if we only focus on the roads to display in the image, there are different possibilities:

- display only the  $n$  closest roads to the interchange point (this is the option chosen in our classification experiment with  $n = 200$ );
- display all the roads that fall into the envelope of the image;

- display only the most important roads;

Figure 18 shows images where we selected only the closest roads with a different number of roads. The threshold of 200 roads was determined empirically, as the classification model trained with these images gave the best classification results. It can be explained by a balance between a good description of the network structure and the complexity of the image.

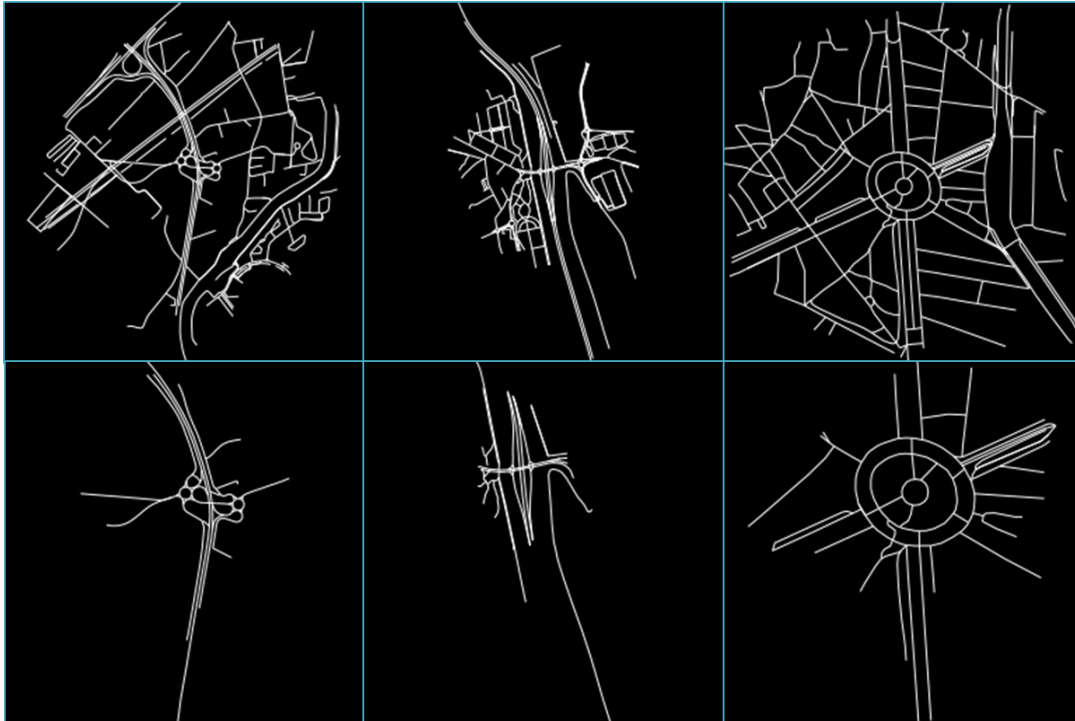


Figure 18: Three areas with a different selection of roads: the 200 closest roads on top, and the 50 closest roads below.

We did not test the last option of data selection, *i.e.* selecting only the important roads. Indeed, a simple filter on the importance attribute was often filtering too much roads, even when only removing the least important roads (the black ones in the colored examples presented in this paper). Road network generalization provides methods to select the most important and salient roads, going beyond a basic semantic filter [22]. It would be very interesting to test the training of the segmentation models with images where the road network was generalized to get rid of the minor roads of the network.

If we broaden the scope of data selection, it is possible to display other types of geographic features in the image. For instance, buildings are rarely built inside interchanges, so we could display the buildings in the image. We did not carry out any experiment with buildings for time reasons, but it would be interesting to verify if it can improve the segmentation results, as the classification results are already very good.

#### 5.4 Segmentation Labels

Regarding the segmentation problem, we tried different types of outputs to learn, all derived from the interchange point in our initial dataset. Figure 19 shows some of the labels we tested before selecting the one presented in Section 4.2. All the method that use the roads in the label were the least effective, compared to the more abstract ones.

We also compared the automatically created labels to labels segmented manually, on a very small number of examples (Figure 20). On this small number of examples, the manually segmented labels allowed much better results than our best automatic method (small black square on white background). Although such results cannot be generalized without experiments, we believe that a large amount of manually segmented would better train the segmentation model, which is not a surprise, but creating such a large manual training dataset is costly.

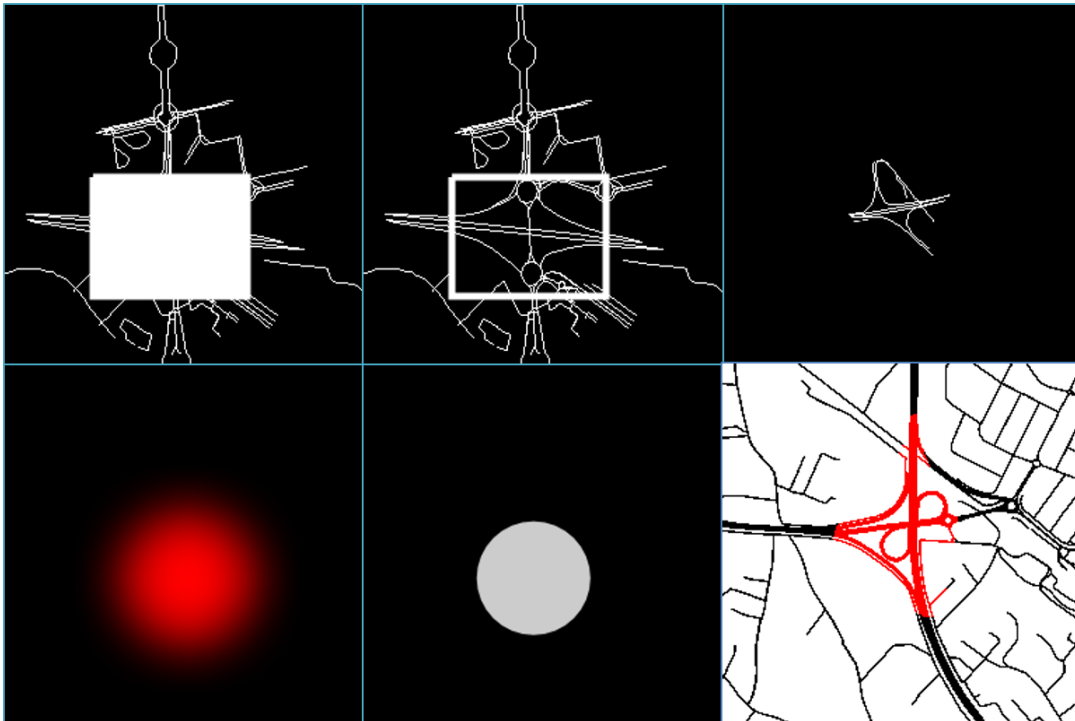


Figure 19: Six alternative methods to generate the label images for the segmentation model.

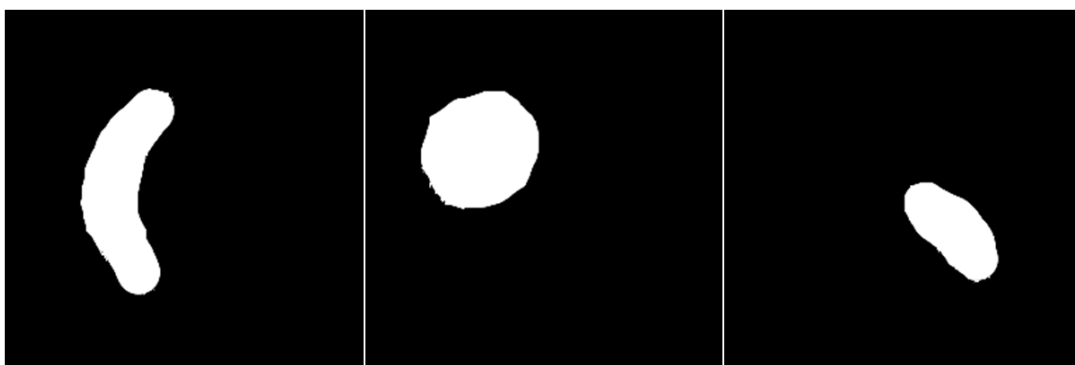


Figure 20: Three examples of label images that were manually segmented.



## 5.5 Data Augmentation

This last sub-section is not strictly about variables to generate training images, but about the possibilities to augment the dataset to have enough training examples. Contrary to photographs, it is very easy to augment a dataset derived from vector by simple translations and rotations during the rasterization. Figure 21 shows an illustration with three images generated for the same interchange point thanks to three different slight translations of the image center from the interchange point.

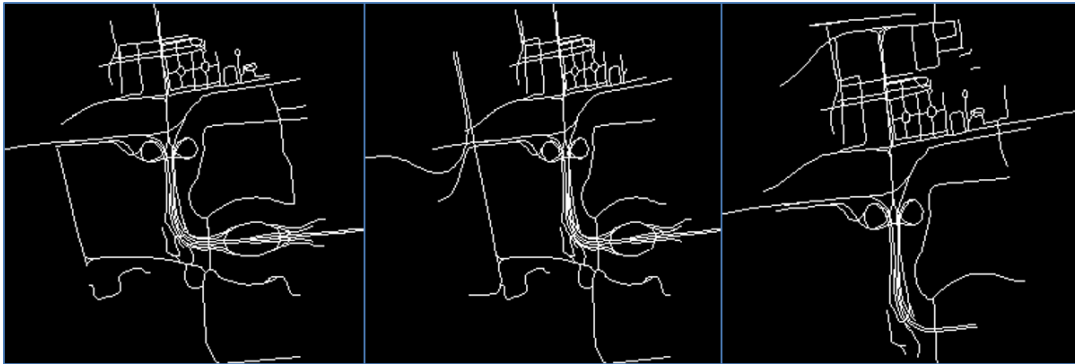


Figure 21: Three images generated from the same interchange point with different translations of the image center from the interchange point.

## 6 Conclusion and Future Work

To conclude, the experiments presented in this paper show that deep learning greatly improves the detection of highway interchanges in vector road data. First, a simple image classification CNN model greatly reduces the number of false positive interchange detection when coupled with the vector-based detection method. Then, the U-Net segmentation model clearly improves the delineation of the interchange roads, even with an automatically generated training dataset. Beyond the progresses on this specific issue, the main contribution of this research is the exploration of different methods to generate images adapted to deep learning models from vector datasets. It opens up new perspectives on the use of deep convolutional networks for pattern recognition with vector spatial data.

There is a lot to do to go further. Regarding the use case on highway interchange, a first step would be to improve the training datasets used for the segmentation model by data augmentation. Another way to improve the training dataset is to use the vector-based method to find interesting areas in the network: it could add new interchange instances that do not have an interchange point in our dataset, and also add false positive cases, *i.e.* areas recognised as interchange by the vector-based method but are not, because it would help the model to learn how to process such cases. Another way to improve the training dataset is to add new instances. We already used all the instances in the French national mapping agency dataset, but we can use the worldwide OpenStreetMap dataset, where the features with the tag value "motorway\_junction" for the tag "highway" (Figure 22). There are different features than the ones used in this paper, but images centered on such features would contain the interchange roads. By the time of writing this paper, there were 171,784 instances<sup>3</sup> of motorway junctions that could be used to generate new examples.

We already mentioned it several times in the paper, but another obvious future work is to improve the vector-based method to obtain optimal results once the roads have been properly filtered by the deep learning models. Our idea is to combine our existing method to the one using road shapes and curvature [18] that also process filtered roads, a semantic filter in their case.

More generally, we can improve the segmentation model by going deeper on the experiments on the model architecture. First, it could be interesting to test residual U-Nets [30] as an improvement of the segmentation model: residual U-Net outperformed traditional U-Nets on different binary segmentation problems. Regarding the loss function, we used a basic binary cross entropy function, and we plan to test more functions such as the one proposed for the seminal U-Net [27] or overlap measures. In order to segment geometrically realistic delineations of the interchanges, it could also be interesting to test generative adversarial networks that perform well to generate realistic map images [2, 31]. We also plan to test the model on other regions of the world that might present other types of interchange patterns. In addition to

<sup>3</sup>[https://wiki.openstreetmap.org/wiki/Tag:highway%3Dmotorway\\_junction](https://wiki.openstreetmap.org/wiki/Tag:highway%3Dmotorway_junction)

these tests on other regions, we want to try the model on other datasets (OpenStreetMap for instance) to check if there are some transfer learning issues.

A straightforward follow-up to this work would be to use deep learning techniques to recognise other types of patterns in road structures, *e.g.* complex crossroads, ring roads, grid-like patterns, or dual carriageways, as existing vector-based methods [14, 15, 17, 19, 18] can really be improved.

A similar approach could also be used for other types of vector analysis problems. For instance, urban block classification is really useful for map generalization purposes but the current approaches based on classical supervised learning techniques fall quite short because the optimal descriptors to classify a building block are not easy to identify. Another interesting example is the inference of landmarks a set of polygon buildings [32, 33]; once again, classical machine learning techniques give perfectible results because it is extremely complex to define the descriptors of what makes a landmark for the human brain.

Finally, one last track for future research would be to generalize the experiments and discussions of Section 5.1: more experiments could help us to define some general guidelines on the variables for image generation (scale, resolution, styling, data selection).

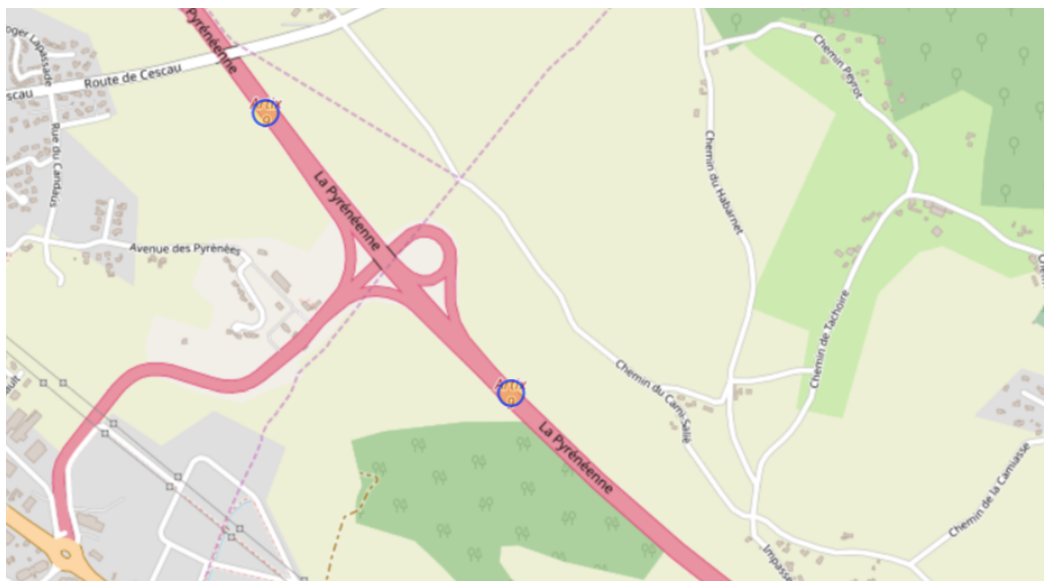


Figure 22: Two OpenStreetMap features with the tag `highway="motorway_junction"` (yellow circle with a blue outline).

## References

- [1] William A. Mackaness and Geoffrey Edwards. The Importance of Modelling Pattern and Structure in Automated Map Generalisation. In *Proceedings of the Joint ISPRS/ICA Workshop on Multi-Scale Representations of Spatial Data*, pages 7–8, 2002.
- [2] Phillip Isola, Jun-Yan Zhu, Tinghui Zhou, and Alexei A. Efros. Image-to-Image Translation with Conditional Adversarial Networks. In *CVPR 2017*, November 2017.
- [3] Torben Peters and Claus Brenner. Conditional Adversarial Networks for Multimodal Photo-Realistic Point Cloud Rendering. In Martin Raubal, Shaowen Wang, Mengyu Guo, David Jonietz, and Peter Kiefer, editors, *Spatial big data and machine learning in GIScience, Workshop at GIScience 2018, Melbourne*, pages 48–53, Melbourne, Australia, 2018. LIPICS.
- [4] Z. Huang, G. Cheng, H. Wang, H. Li, L. Shi, and C. Pan. Building extraction from multi-source remote sensing images via deep deconvolution neural networks. In *2016 IEEE International Geoscience and Remote Sensing Symposium (IGARSS)*, pages 1835–1838, July 2016.
- [5] Nicolas Audebert, Bertrand Le Saux, and Sebastien Lefevre. Joint Learning from Earth Observation and OpenStreetMap Data to Get Faster Better Semantic Maps. In *2017 IEEE Conference on Computer Vision and Pattern Recognition Workshops (CVPRW)*, pages 1552–1560, Honolulu, HI, USA, July 2017. IEEE.

- [6] Loïc Landrieu and Martin Simonovsky. Large-scale Point Cloud Semantic Segmentation with Superpoint Graphs. In *Conference on Computer Vision and Pattern Recognition (CVPR)*, Salt Lake City, Utah, USA, June 2018.
- [7] Jiaoyan Chen and Alexander Zipf. DeepVGI: Deep Learning with Volunteered Geographic Information. In *Proceedings of the 26th International Conference on World Wide Web Companion - WWW '17 Companion*, pages 771–772, Perth, Australia, 2017. ACM Press.
- [8] R. F. Berriel, A. T. Lopes, A. F. de Souza, and T. Oliveira-Santos. Deep Learning-Based Large-Scale Automatic Satellite Crosswalk Classification. *IEEE Geoscience and Remote Sensing Letters*, 14(9):1513–1517, September 2017.
- [9] Tristan Postadjian, Arnaud Le Bris, Hichem Sahbi, and Clément Mallet. Domain adaptation for large scale classification of very high resolution satellite images with deep convolutional neural networks. In *2018 IEEE International Geoscience and Remote Sensing Symposium, IGARSS 2018, Valencia, Spain, July 22-27, 2018*, pages 3623–3626, 2018.
- [10] Yongyang Xu, Zhanlong Chen, Zhong Xie, and Liang Wu. Quality assessment of building footprint data using a deep autoencoder network. *International Journal of Geographical Information Science*, 31(10):1929–1951, October 2017.
- [11] Y Méneroux, V Dizier, M Margollé, M D Van Damme, Y Kato, A Le Guilcher, and Guillaume Saint-Pierre. Convolutional Neural Network for Road Sign Inference based on GPS Traces. In *Spatial Big Data and Machine Learning in GIScience, Workshop at GIScience 2018*, page 4, Melbourne, Australia, 2018.
- [12] M. Sester, Y. Feng, and F. Thiemann. Building Generalization Using Deep Learning. *ISPRS - International Archives of the Photogrammetry, Remote Sensing and Spatial Information Sciences*, XLII-4:565–572, October 2018.
- [13] Guillaume Touya, Xiang Zhang, and Imran Lokhat. Is Deep Learning the New Agent for Map Generalization? *International Journal of Cartography*, 5, 2019.
- [14] Q. Zhang. Modelling Structure and Patterns in Road Network Generalization. In *ICA Workshop on Generalisation and Multiple Representation*, August 2004. event-place: Leicester, UK.
- [15] Frauke Heinzle, Karl-Heinrich Anders, and Monika Sester. Graph Based Approaches for Recognition of Patterns and Implicit Information in Road Networks. In *International Cartographic Conference*. ICA, 2005. event-place: La Coruña, Spain.
- [16] Robert C. Thomson. The 'stroke' concept in geographic network; generalization and analysis. In Andreas Riedl, Wolfgang Kainz, and Gregory A. Elmes, editors, *Progress in Spatial Data Handling 12th International Symposium on Spatial Data Handling*, pages 681–697. 2006.
- [17] Frauke Heinzle and Karl-Heinrich Anders. Characterising Space via Pattern Recognition Techniques: Identifying Patterns in Road Networks. In William A. Mackaness, A. Ruas, and T. Sarjakoski, editors, *The Generalisation of Geographic Information : Models and Applications*. Elsevier, 2007.
- [18] Sandro Savino, M. Rumor, M. Zanon, and I. Lissandron. Data enrichment for road generalization through analysis of morphology in the CARGEN project. In *Proceedings of 13th ICA Workshop on Generalisation and Multiple Representation*, Zurich, Switzerland, 2010.
- [19] Bisheng Yang, Xuechen Luan, and Qingquan Li. An adaptive method for identifying the spatial patterns in road networks. *Computers, Environment and Urban Systems*, 34(1):40–48, January 2010.
- [20] Ahmet Ozgur Dogru, Nico Van de Weghe, Necla Ulugtekin, and Philippe De Maeyer. Classification of road junctions based on multiple representations: adding value by introducing algorithmic and cartographic approaches. In *Proceedings of the International Cartographic Conference*, Moscow, Russia, 2007.
- [21] William A. Mackaness and Gordon A. Mackechnie. Automating the Detection and Simplification of Junctions in Road Networks. *Geoinformatica*, 3(2):185–200, 1999.
- [22] Guillaume Touya. A Road Network Selection Process Based on Data Enrichment and Structure Detection. *Transactions in GIS*, 14(5):595–614, 2010.
- [23] Stuart Thom. A Strategy for Collapsing OS Integrated Transport Network Dual Carriageways. In *8th ICA Workshop on Generalisation and Multiple Representation*, La Coruña, Spain, 2005.
- [24] Y. Lecun, L. Bottou, Y. Bengio, and P. Haffner. Gradient-based learning applied to document recognition. *Proceedings of the IEEE*, 86(11):2278–2324, November 1998.
- [25] Nitish Srivastava, Geoffrey Hinton, Alex Krizhevsky, Ilya Sutskever, and Ruslan Salakhutdinov. Dropout: A simple way to prevent neural networks from overfitting. *Journal of Machine Learning Research*, 15:1929–1958, 2014.

- [26] Ramprasaath R. Selvaraju, Michael Cogswell, Abhishek Das, Ramakrishna Vedantam, Devi Parikh, and Dhruv Batra. Grad-CAM: Visual Explanations from Deep Networks via Gradient-based Localization. *arXiv:1610.02391 [cs]*, October 2016. arXiv: 1610.02391.
- [27] Olaf Ronneberger, Philipp Fischer, and Thomas Brox. U-Net: Convolutional Networks for Biomedical Image Segmentation. *CoRR*, abs/1505.04597, 2015.
- [28] *DeepLab: Semantic Image Segmentation with Deep Convolutional Nets, Atrous Convolution, and Fully Connected CRFs*. May 2017.
- [29] Joseph Redmon, Santosh Kumar Divvala, Ross B. Girshick, and Ali Farhadi. You Only Look Once: Unified, Real-Time Object Detection. In *CVPR 2016*, 2016.
- [30] Z. Zhang, Q. Liu, and Y. Wang. Road Extraction by Deep Residual U-Net. *IEEE Geoscience and Remote Sensing Letters*, 15(5):749–753, May 2018.
- [31] Yuhao Kang, Song Gao, and Robert E. Roth. Transferring Multiscale Map Styles Using Generative Adversarial Networks. *International Journal of Cartography*, 2019.
- [32] Birgit Elias. Extracting Landmarks with Data Mining Methods. In Werner Kuhn, Michael F. Worboys, and Sabine Timpf, editors, *Spatial Information Theory. Foundations of Geographic Information Science*, volume 2825 of *Lecture Notes in Computer Science*, pages 375–389. Springer Berlin Heidelberg, 2003.
- [33] Guillaume Touya and Marion Dumont. Progressive Block Graying and Landmarks Enhancing as Intermediate Representations between Buildings and Urban Areas. In *Proceedings of 20th ICA Workshop on Generalisation and Multiple Representation*, Washington DC, USA, July 2017.